JOURNAL OF CHEMICAL INFORMATION AND MODELING

Article

pubs.acs.org/jcim

A Possible Mechanism for Redox Control of Human Neuroglobin Activity

Alexander N. Morozov,* James P. Roach, Margarita Kotzer, and David C. Chatfield*

Department of Chemistry and Biochemistry, Florida International University, Miami, Florida 33199, United States

Supporting Information

ABSTRACT: Neuroglobin (Ngb) promotes neuron survival under hypoxic/ischemic conditions. *In vivo* and *in vitro* assays provide evidence for redox-regulated functioning of Ngb. On the basis of X-ray crystal structures and our MD simulations, a mechanism for redox control of human Ngb (hNgb) activity via the influence of the CD loop on the active site is proposed. We provide evidence that the CD loop undergoes a strand-to-helix transition when the external environment becomes sufficiently oxidizing, and that this CD loop conformational transition causes critical restructuring of the active site. We postulate that the strand-to-helix mechanics of the CD loop allows hNgb to utilize the lability of Cys46/Cys55 disulfide bonding and of the Tyr44/His64/heme propionate interaction network for redox-controlled functioning of hNgb.

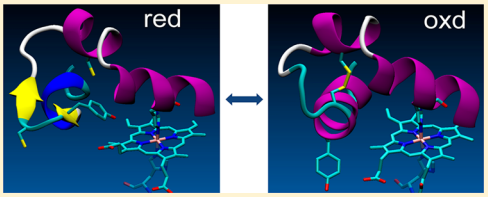

Neuroglobin (Ngb) is a monomeric globin expressed in the central and peripheral nervous systems of vertebrates.[1] In the course of mammalian evolution, the amino acid sequence of Ngb has been strongly conserved,[2] suggesting an important physiological function not yet understood. Myoglobin (Mb) and hemoglobin (Hb), discovered much earlier, are globin families functioning mainly as oxygen storage/transport proteins. The sequence of Ngb is less than 25% homologous with that of Mb or Hb.[1,3] Presumably this difference is a result of evolutionary pressure toward a distinct function. Despite the difference in the primary sequences, the tertiary fold of Ngb is essentially the same as that of Mb or Hb,[3] i.e., the classical 3-over-3 α-helical frame for binding the heme prosthetic group. Heme binding to apoproteins of Mb or Hb is coordinated by the proximal histidine in the F helix, and thus, the deoxy state of these globins has a pentacoordinated heme iron. Ngb is different as both the ferrous (Fe^{2+}) and ferric (Fe^{3+}) deoxy states are characterized by a hexacoordinated heme iron with the penta and hexa bonds formed by the proximal histidine (His96) in the F helix and by the distal histidine (His64) in the E helix, respectively.[4] The His64−iron bond undergoes a reversible dissociation, thereby allowing diatomic gaseous ligands to compete for the iron.[4,5] Reversible hexacoordination also occurs in plant, bacterial, and invertebrate globins, implicating a biological utility of this phenomenon. The specific biological purpose of hexacoordination is not clear, although in general, it is thought to be related to the modulation of gaseous ligand affinities or electron transfer rate.[6,7] Another peculiar feature of Ngb is a large internal cavity in the protein interior, on the opposite side of the heme from the CD loop.[3,8] This cavity, a costly packing defect not observed in Mb,[9] is utilized by murine Ngb in its heme sliding mechanism.[10] Ngb's heme sliding could be an alternative to Mb's his-gate mechanism[11] for the control of ligand affinity and ligand migration.[9,10,12] Heme sliding, however, may be a species-specific phenomenon as suggested by theoretical studies of human Ngb.[13,14]

In vitro and *in vivo* assays show that elevated levels of Ngb protect neural tissues under hypoxic and ischemic conditions.[15−18] The neuroprotective effect of Ngb upon acute brain injury can last for up to 2 weeks.[17] It is expected that modulation of Ngb expression may significantly advance stroke treatment strategies. The physiological evidence of Ngb's role in the cell revolves around the oxygen storage function, reactive oxygen species (ROS) metabolism, redox sensing/signaling, and inhibition of apoptosis.[19] Ngb is expressed within cell zones having the highest oxygen requirement.[1,19,20] Although Ngb does not reside within mitochondria, the expression data show that Ngb is colocalized with this organelle.[20,21] It has been established that under hypoxic conditions mitochondria elevate release of ROS.[22] Thus, it is likely that hypoxia-induced release of mitochondrial ROS initiates a cellular redox process whereby Ngb's neuroprotective function is up-regulated.[23] In the case of human Ngb (hNgb), this postulate is supported by experimental evidence that under oxidizing conditions hNgb has higher affinities for gaseous ligands[24,25] and higher enzymatic activity.[23,26] In particular, hNgb's nitrite reductase activity displays a sigmoidal dependence on the redox potential of the solution (Figure 2 in ref 23.). This implies that hNgb possesses a redox-regulated switch, essentially a post-translational structure/function modification. A pair of cysteine residues, Cys46 and Cys55, located on the surface of hNgb in the loop between the C and D helices (CD loop) and in the N-terminal end of the short D helix,[3] was identified for this role. The Cys46Gly/Cys55Ser mutation and the reduction of the Cys46/Cys55 disulfide bond have similar effects on the oxygen affinity of hNgb.[24] The nitrite reductase activity of the Cys55Ala mutant of hNgb displays no dependence on the

Published: May 25, 2014

   dx.doi.org/10.1021/ci5002108 | *J. Chem. Inf. Model.* 2014, 54, 1997−2003

Table 1. Selected Distances (Å) from 1OJ6 Crystal and Corresponding MD Averages

	46:Ca - 55:Ca	44:O - 47:N	44:N - 47:O	42:O - 49:N	42:O - 46:N	41:O - 45:N	40:O - 44:N	39:O - 43:N	38:O - 42:N
1OJ6 A[a]	13.3	5.0	3.2	4.5	7.6	10.1	7.3	6.0	4.0
1OJ6 B	14.0	2.9	3.4	4.6	8.1	9.9	7.6	5.7	4.3
1OJ6 C	14.1	2.7	3.4	4.6	7.9	9.9	7.5	5.9	4.3
1OJ6 D[a]	9.0	8.1	7.5	8.9	5.9	7.5	4.9	4.1	4.2
Cys120Ser[b] $hNgb_{red}$	13 ± 0.6	3.4 ± 0.3	3.5 ± 0.5	5.0 ± 0.3	8.5 ± 0.5	9.8 ± 0.5	7.9 ± 0.5	5.5 ± 0.5	3.7 ± 0.4
WT $hNgb_{red}$	13 ± 0.7	3.4 ± 0.4	3.6 ± 0.6	4.8 ± 0.5	8.4 ± 0.5	9.8 ± 0.5	7.8 ± 0.5	5.5 ± 0.5	3.9 ± 0.5
Cys120Ser $hNgb_{ox}$	5.5 ± 0.2	5.0 ± 1.1	7.6 ± 1.4	8.3 ± 0.8	3.5 ± 0.4	3.8 ± 0.6	3.4 ± 0.5	3.0 ± 0.2	3.1 ± 0.2
WT $hNgb_{ox}$	5.2 ± 0.2	3.5 ± 0.6	6.9 ± 0.2	6.8 ± 0.3	3.0 ± 0.2	5.5 ± 0.3	5.3 ± 0.4	3.1 ± 0.2	3.3 ± 0.4

[a]Tyr44 side chain was not resolved. [b]Averaged over 0−30 and 80−100 ns (Figure 3).

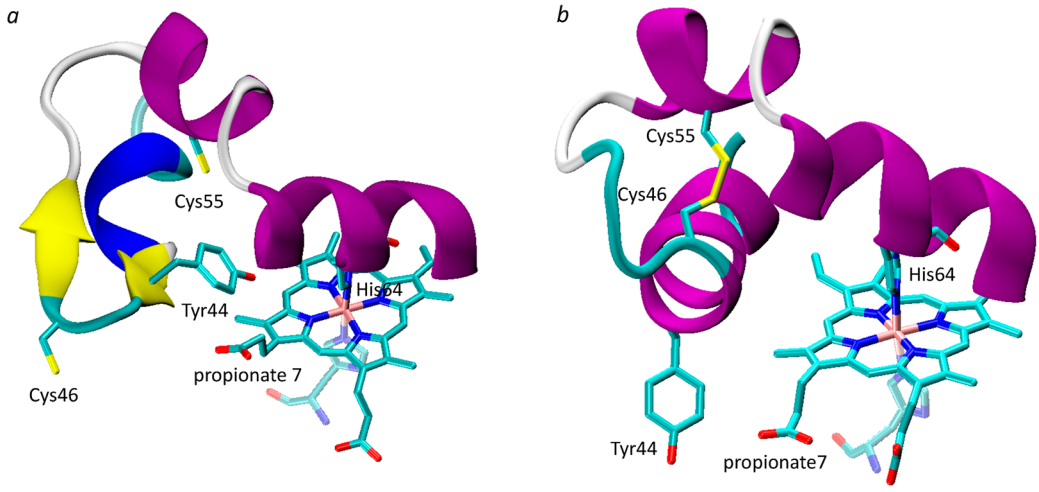

Figure 1. MD snapshots: Residue 37−67 fragment of hNgb and bis-His-coordinated heme are shown. (a) CD_{str} state: Residues 42−49 of CD loop form a strand; Tyr44 is bound to the distal pocket. (b) CD_{hx} state: Residues 42−46 of CD loop form a helix; Tyr44 binding to the distal pocket is ruptured.

solution redox state.[23] Analysis of the rebinding kinetics of the CO ligand photodissociated from the heme iron showed that formation of the Cys46/Cys55 disulfide bond is paralleled by a 10-fold increase in the His64−iron dissociation rate.[24] Thus, a general concept for the redox-regulated functioning of hNgb emerges: hNgb's interactions with external ligands are regulated by the local redox state of the cytoplasm through the effect of the rupture/formation of the Cys46/Cys55 disulfide bond on the association/dissociation rate of the heme iron−distal histidine bond.

The molecular mechanism underlying such postulated functioning is not well understood. Opportunities for an oxidation event resulting in disulfide formation exist *in vivo*, for example, when ROS released by mitochondria reach the surface of hNgb. A first hint about the subsequent chain of events that could lead to functional switching was gleaned from examination of the X-ray structure 1OJ6 of the Cys46Gly/Cys55Ser/Cys120Ser triple mutant of hNgb.[3] In the four monomers (A, B, C, and D) of the tetrameric 1OJ6 crystal structure, the alpha carbons (C_α) of residues 46 and 55 are separated by distances ranging from 9 to 14 Å (Table 1).[3] Assuming that the structures of the 1OJ6 monomers are representative of reduced wild type hNgb ($hNgb_{red}$, i.e., without the Cys46/Cys55 disulfide bond), it appears that the spatial separation of residues 46 and 55 in $hNgb_{red}$ precludes Cys46/Cys55 disulfide bond formation.[24] Thus, one might consider rearrangement of the CD loop to create a conformational precursor to Cys46/Cys55 bond formation to be the first step toward modification of $hNgb_{red}$ into oxidized hNgb ($hNgb_{ox}$, i.e., with the Cys46/Cys55 disulfide bond present). This conformational precursor would be readily converted to $hNgb_{ox}$. For functional switching to occur, the CD loop conformation with the Cys46/Cys55 disulfide bond present must exert influence on the active site. The 1OJ6 structure provides a hint about how this happens as well. Monomers B and C possess a clearly resolved Tyr44 side chain, positioned so as to influence small ligand access to the active site and the conformational ensemble of His64. In monomers A and D, the Tyr44 side chain is unresolved; these are also the monomers with the smaller Cys46/Cys55 C_α−C_α distances. Thus, the 1OJ6 crystal structure provides hints of a correlation between the CD loop conformation and Tyr44/distal pocket interactions.

Motivated by these observations, we sought clues to the molecular mechanism of the redox-dependent functioning of hNgb by probing hNgb for a conformational precursor to Cys46/Cys55 disulfide bond formation and by examining hNgb structural modifications induced by Cys46/Cys55 disulfide bond formation, using molecular dynamics (MD) simulation with appropriate restraint and annealing methods (techniques are described in context below; see Supporting Information for full details). The results presented here show that the CD loop samples two conformational states with characteristic strand (CD_{str}) and helical (CD_{hx}) structural motifs (Figure 1). Below, we provide arguments that hNgb utilizes two-state CD loop mechanics to sense the redox state of the cytoplasm and to respond, via a structure/function switch, to changes in this redox state.

STRAND STATE OF CD LOOP UNDER EXTERNAL REDUCING CONDITIONS

The CD_{str} state (Figure 1a), which manifests a beta turn and a short distorted beta strand formed in the residue 42−49 region, is revealed in monomers B and C of the 1OJ6 crystal structure[3] and in the X-ray structures of murine Ngbs.[8,27] Because they lack one or both of the CD loop cysteines, these Ngb structures do not have the ability to form a disulfide bond in the CD loop region, and thus, they represent conformations hNgb may favor under external reducing conditions. We performed 100 ns MD simulations of the reduced forms of wild type (WT) hNgb and of the Cys120Ser mutant of hNgb in explicit aqueous solvent. These simulations confirm that the CD_{str} state of the CD loop is stable not only in the crystal environment but also in solution at ambient temperatures. The stability of CD_{str} depends on a pair of backbone hydrogen bonds formed between residues Tyr44 and Arg47, a transient backbone hydrogen bond between residues Phe42 and Phe49, and a network of interactions involving the Tyr44 side chain (Figure 2). The

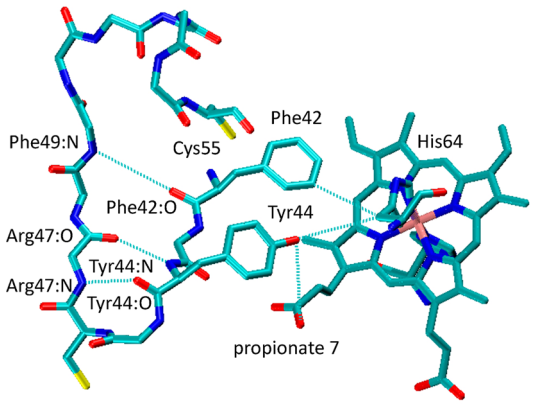

Figure 2. MD snapshot: CD_{str} network and Phe42/His64 steric contact are shown.

latter moiety exhibits favorable steric and electrostatic interactions with the His64 side chain and interacts with heme propionate 7 either directly with a hydrogen bond or indirectly via a water bridge. Along with Tyr44/His64 interactions, in the CD_{str} state, the distal histidine also maintains van der Waals' contact with the side chain of CD loop residue Phe42 (Figure 2). It should be noted that Phe42 is an evolutionarily conserved residue in the globin family, while Tyr44 has functional analogues in both Mb and Hb.[1,3] The time evolutions of key interatomic distances pertaining to the strand backbone hydrogen bonding are shown in Figure 3b−d; corresponding statistics are given in Table 1.

STRAND-TO-HELIX REARRANGEMENT CREATES A DISULFIDE BOND PRECURSOR

The MD simulations of $hNgb_{red}$ showed that in the CD_{str} state, the distance between the sulfur atoms of Cys46 and Cys55 pair fluctuates around 15 Å. Using MD at an elevated temperature (CD loop flexible, rest of protein constrained) with a combination of sulfur−sulfur distance restraints and orientational restraints on the Cys46 and Cys55 side chains, these two cysteine residues were gradually brought close to each other, resulting in a conformational precursor to disulfide bond formation. We observed that such a precursor conformation is created when residues 42 to 46 of the CD loop undergo a *strand-to-helix rearrangement* (Figure 3) *concomitant with a rupture of the Tyr44 interaction network* (Figure 4c,d). The strand-to-helix rearrangement of the CD loop shortens the distance between residues 42 and 46, thereby bringing residues 46 and 55 close enough to create a precursor conformation for disulfide bond formation (Figure 5). Incipient strand-to-helix rearrangement is sampled through elongation of the C helix [see periods 30−80 (during unrestrained MD of Cys120Ser) and 100−110 ns (during restrained MD) in Figure 3]. Rupture of the Tyr44/His64/propionate 7 network is prerequisite to reaching the disulfide precursor conformation. This observation from MD simulation is supported by examination of monomers A and D of the 1OJ6 crystal structure, in which the Tyr44 side chain is unresolved and the beta-strand hydrogen-bond interactions are weakened, suggesting that disruption of the Tyr44 interaction network accompanies structural disorder in the strand (Table 1). Monomer D is particularly supportive of our interpretation of the MD results, as the Cys46/Cys55 C_α−C_α distance is relatively small (9 Å vs ∼14 Å for the other monomers), and the side chain of residue 55 is oriented toward residue 46. Comparison of monomer D with monomers A, B, and C and with our MD results (Table 1, Figure 5) confirms that a decrease in the Cys46/Cys55 C_α−C_α distance is achieved through a strand-to-helix conformational transition concomitant with rupturing of the Tyr44 interaction network.

HELICAL STATE OF CD LOOP UNDER EXTERNAL OXIDIZING CONDITIONS

When in the presence of an external oxidizing environment, a conformational precursor is converted to the Cys46/Cys55 cystine form; the CD_{hx} state of the CD loop is stabilized. Such an oxidation event was modeled by beginning with a conformational precursor and applying appropriate parameters to the Cys46 and Cys55 residues to create a disulfide bond. The CD loop region was annealed, keeping the rest of the protein constrained. After relaxation and equilibration of the protein, the initial $hNgb_{ox}$ structure was obtained. In 100 ns MD simulations of WT $hNgb_{ox}$ and of the Cys120Ser mutant $hNgb_{ox}$, the CD_{hx} state demonstrated stability (Table 1, Figure 3e−i). The helical structural motif is clearly present in the residue 42−46 region of the CD loop in both simulations. However, in the last turn of the helix for the WT trajectory, the Pro40:O/Tyr44:N and Leu41:O/Asn45:N backbone hydrogen bonds were twisted (Table 1). The CD_{hx} state should be viewed then as a collection of metastable CD loop conformers whose diversity stems from perturbations by the surrounding environment but whose essential structure results from the backbone attraction of residues 42−46 into the helical potential basin.

The MD simulations of $hNgb_{ox}$ also revealed structural changes in the distal pocket caused by the CD_{str}-to-CD_{hx} transition. First, in both the WT and Cys120Ser mutant $hNgb_{ox}$ simulations, the Tyr44 side chain was displaced out of the distal pocket, and consequently, the Tyr44/His64 interaction was permanently lost (Figure 4c). In the Cys120Ser $hNgb_{ox}$ trajectory, the Phe42 side chain was also reoriented, with loss of the Phe42/His64 close contact (Figure 4b). The observed difference in the WT and Cys120Ser evolutions of the Phe42−His64 distance is likely due to sampling limitations rather than to mutation. With loss of the Tyr44/His64 and Phe42/His64 contacts, thermal excitations of the His64 side chain would have an increased likelihood of dissipating through dissociation of the His64/iron bond. Second, we observed that

dx.doi.org/10.1021/ci5002108 | J. Chem. Inf. Model. 2014, 54, 1997−2003

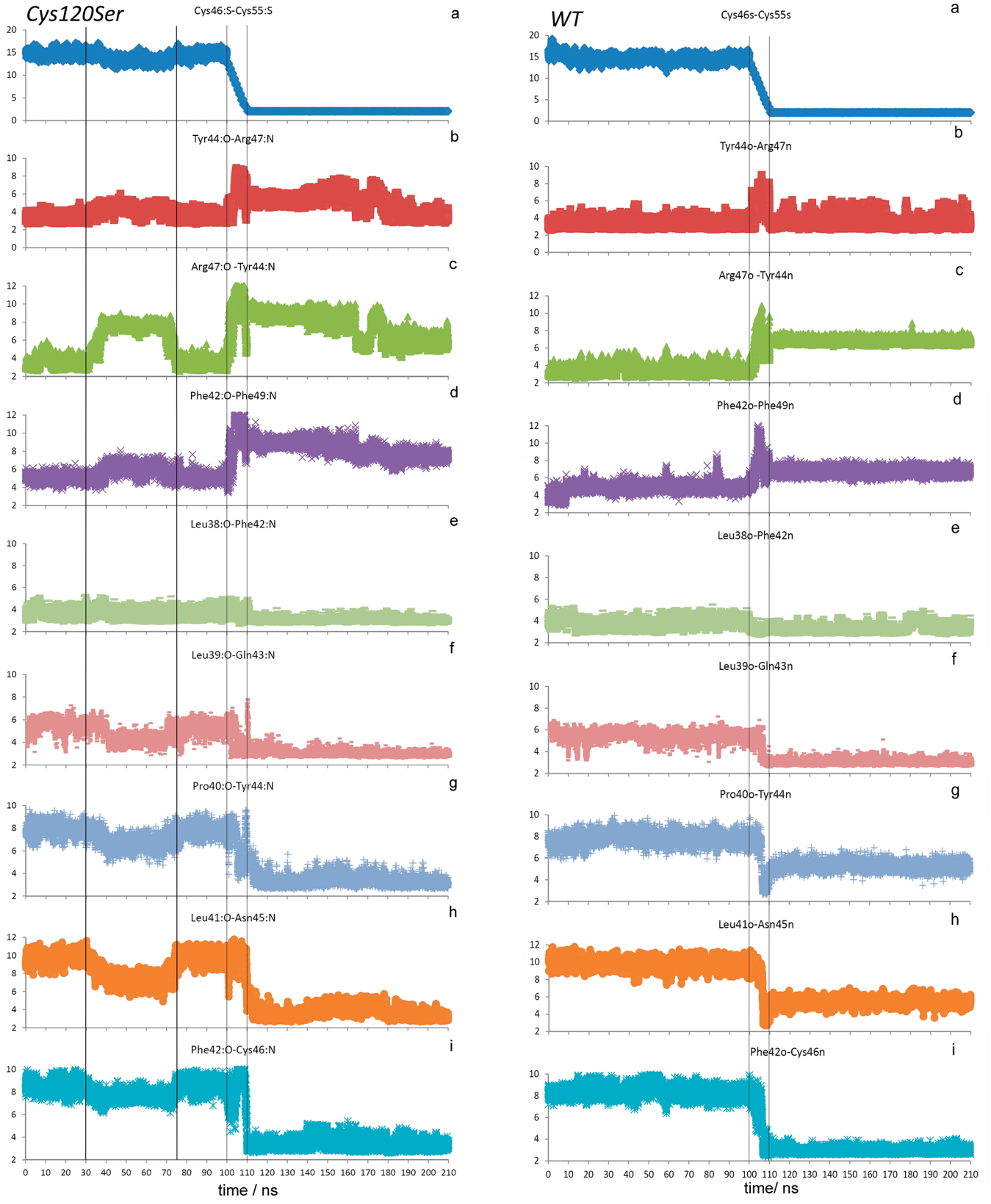

Figure 3. Strand-to-helix transition: Cys120Ser (left panel); WT (right panel). The strand or helical state of the CD loop is determined based on the presence of corresponding backbone hydrogen bonds (see Supporting Information for details). *Y*-axis: distances in Å. *X*-axis: 0−100 ns, $hNgb_{red}$; 100−110 ns, restrained MD, to form first the conformational precursor and then the disulfide bond; and 110−210 ns, $hNgb_{ox}$ simulations. (a) Cys46/Cys55 disulfide evolution. (b−d) Time evolution of strand backbone hydrogen bonding. (e−i) Time evolution of helical backbone hydrogen bonding. Black solid lines are to guide the eye for the period of the transient strand-to-helix transition during simulation of the reduced form. Gray solid lines indicate the period of restrained MD during which the oxidized form is created.

dx.doi.org/10.1021/ci5002108 | *J. Chem. Inf. Model.* 2014, 54, 1997−2003

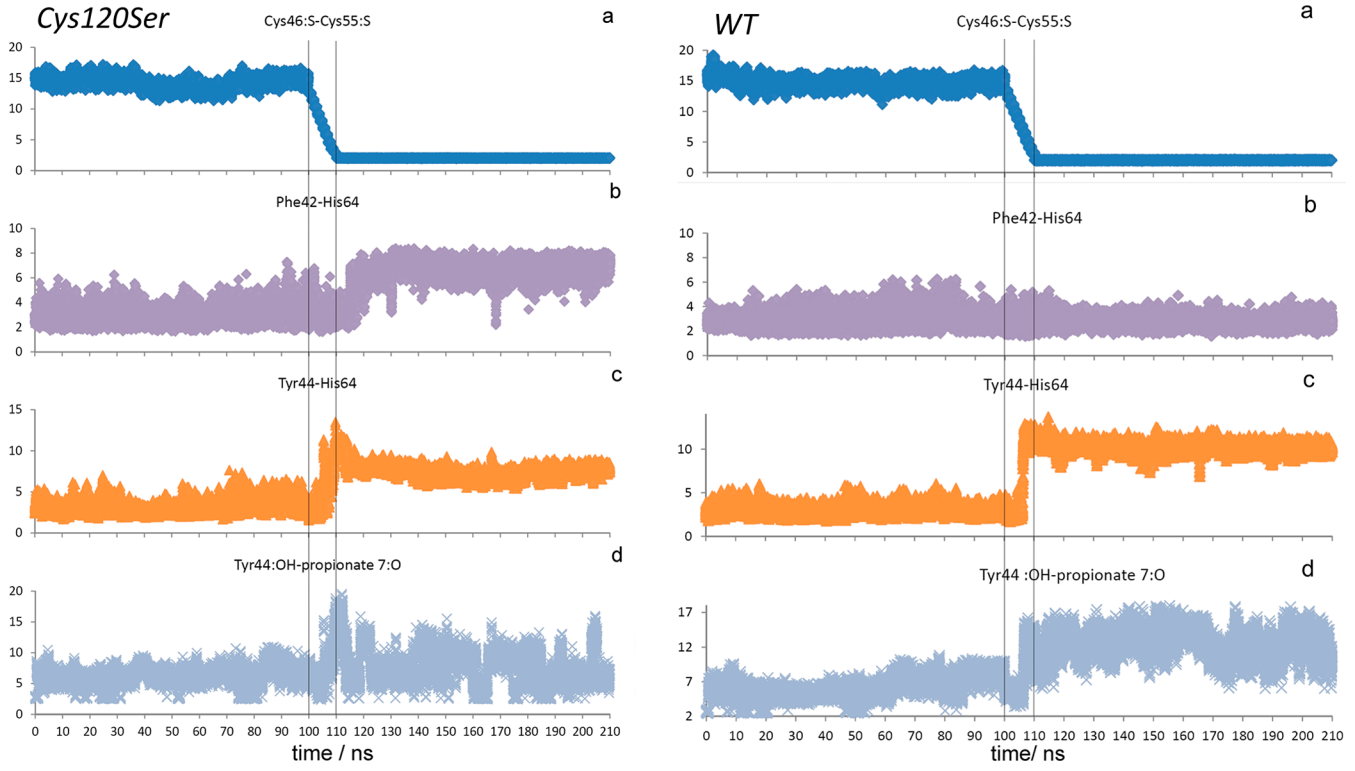

Figure 4. Effect of CD loop transition on the distal pocket: Cys120Ser (left panel); WT (right panel). *Y*-axis: Distances in Å. (a) Cys46/Cys55 disulfide evolution. (b,c) Minimum distance between side chains of His 64 and of Phe42 and Tyr44, respectively. (d) Minimum distance between side chain oxygen of Tyr44 and oxygen atoms of heme propionate 7. Note that in $hNgb_{ox}$,Tyr44 interacts with the propionate 7 on the proximal side of the heme (Figure 1b). The vertical lines are to guide the eye as described in the caption for Figure 3.

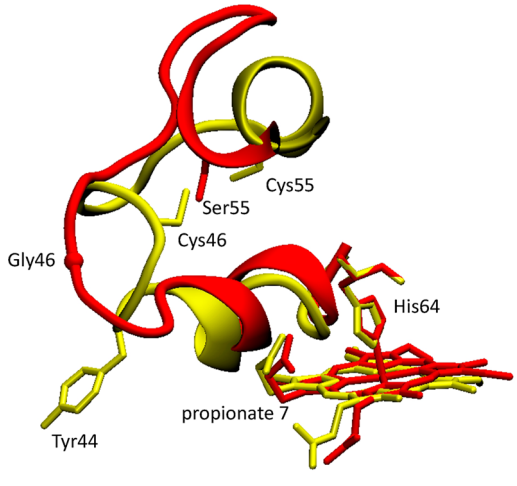

Figure 5. Overlap of CD fragments from 1OJ6 monomer D (red, Tyr44 side chain not resolved) and of a snapshot from Cys120Ser simulations of the disulfide precursor (yellow: distance between sulfur atoms of residues Cys46 and Cys55 is 2.95 Å).

the disturbance of Tyr44 interactions with His64 and propionate 7 evolves into a gating motion that opens a channel communicating the distal pocket active center directly to the solvent exterior near the CD loop corner (Figure 6). Known as the "distal histidine gate pathway",[11] this channel is postulated to be the fast route for access of an exogenous ligand to the active center of Mb.[28,29] Otherwise, an exogenous ligand has to diffuse through an intricate system of internal cavities and gates starting near the AB, GH, or EF hinges.[14,29−31] In summary, the distal pocket modifications observed in the simulations of $hNgb_{ox}$ would be expected to increase the rate of dissociation of the distal histidine and to facilitate access of an exogenous ligand to the active center of hNgb.

REDOX CONTROL MECHANISM

On the basis of the factors outlined above, we postulate that the mechanism for redox control of hNgb activity functions as follows. The CD loop samples strand and helical conformational states via elongation of the C helix into the residue 42−46 region. Under reducing conditions, the strand state is favored by a Tyr44 interaction network in which the Tyr44 side chain blocks external ligands from direct access to the active center and together with the Phe42 side chain hinders His64 mobility. However, the residue 42−46 region visits the helical state transiently, which requires disruption of the Tyr44 interaction network. Upon such a visit, a conformational precursor of the $hNgb_{ox}$ state is created as the strand-to-helix transition shortens the distance between residues Cys46 and Cys55. This allows hNgb to sense the redox state of the external environment. Under reducing conditions, the CD loop returns to the strand state. Under oxidizing conditions, the conformational precursor is converted to $hNgb_{ox}$ by formation of the Cys46/Cys55 disulfide bond, and the helical state of the CD loop becomes stabilized. The distal pocket is altered in several ways by this CD loop rearrangement, with removal of the Tyr44 side chain from the distal pocket being particularly significant. As a result of these changes, hindrance of His64 mobility by the Tyr44 side chain and probably also by the Phe42 side chain is removed, and the rate of dissociation of the His64−iron bond is increased. Also, the rupture of the Tyr44 interactions with the distal histidine and heme propionate 7

dx.doi.org/10.1021/ci5002108 | J. Chem. Inf. Model. 2014, 54, 1997−2003

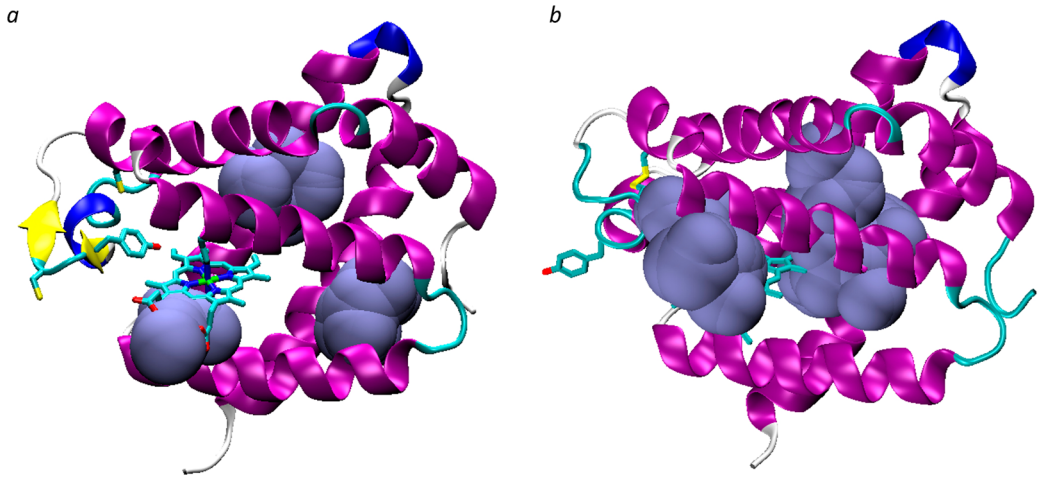

Figure 6. Cavity analysis of average hNgb structures over 100 ns. (a) $hNgb_{red}$ shows good agreement with the experimental xenon cavities.[30] (b) Distal pathway communicating the active center directly to the solvent exterior is opened in $hNgb_{ox}$.

facilitates exogenous ligand access to the active center by opening the direct "distal pathway" channel connecting the active center with the solvent exterior. In summary, we postulate that the *strand-to-helix* mechanics of the CD loop allows hNgb to utilize the lability of Cys46/Cys55 disulfide bonding and of the Tyr44/His64/propionate 7 interaction network for (i) functioning as a sensor of the redox state of the cytoplasm and (ii) for modulating ligand binding affinity and enzymatic activity in response to a change in the cytoplasm's redox state.

After this manuscript was completed, a new crystal structure of WT hNgb (pdb 4MPM) was published.[32] This structure is a dimer with the disulfide bond present in each monomer. Both of the 4MPM subunits have (i) the Phe42 side chain displaced relative to the 1OJ6 structure, (ii) the Tyr44 side chain outside of the distal pocket, and the Tyr44/His64/propionate 7 network absent, and (iii) an internal cavity enclosed by the CD loop and connected to the distal pocket. In chain A of 4MPM, the C helix is significantly elongated, the Tyr44 side chain is facing the solvent exterior, and the CD loop cavity is a part of the direct "distal pathway" channel reported here. In chain B of 4MPM, the C helix elongation is slighter and distorted, the Tyr44 side chain is directed toward propionate 7, and the CD loop cavity partially overlaps with our direct "distal pathway" channel. The 4MPM X-ray structure[32] provides experimental evidence of the mechanism for redox control of human neuroglobin activity postulated in this letter, while also raising questions about the possible role of CD loop flexibility[32] and the relative stability of the different CD loop and key active site residue conformations in $hNbg_{ox}$ state.

■ ASSOCIATED CONTENT

Supporting Information

MD simulation methods and details, force field parameters for low spin ferrous bis-His hexacoordinated heme, and the structure of the CD_{hx} state for WT hNgb. This material is available free of charge via the Internet at http://pubs.acs.org.

■ AUTHOR INFORMATION

Corresponding Authors

*E-mail: omorozov@fiu.edu.
*E-mail: David.Chatfield@fiu.edu.

Present Address

J.P.R.: Neuroscience Graduate Program, University of Michigan, Ann Arbor, MI 48109.

Author Contributions

A.N.M and J.P.R: These authors contributed equally.

Author Contributions

The manuscript was written through contributions of all authors. All authors have given approval to the final version of the manuscript.

Notes

The authors declare no competing financial interest.

■ ACKNOWLEDGMENTS

We thank Dr. Jaroslava Miksovska for helpful conversations. We acknowledge the Instructional & Research Computing Center (IRCC) at Florida International University for providing computing resources. This work was supported by an NIGMS MARC U*Star fellowship to J.P.R. and NIH Grant SC3GM083723 to D.C.C.

■ REFERENCES

(1) Burmester, T.; Weich, B.; Reinhardt, S.; Hankeln, T. A vertebrate globin expressed in the brain. *Nature* **2000**, *407*, 520−523.

(2) Burmester, T.; Haberkamp, M.; Mitz, S.; Roesner, A.; Schmidt, M.; Ebner, B.; Gerlach, F.; Fuchs, C.; Hankeln, T. Neuroglobin and cytoglobin: Genes, proteins and evolution. *IUBMB Life* **2004**, *56*, 703−707.

(3) Pesce, A.; Dewilde, S.; Nardini, M.; Moens, L.; Ascenzi, P.; Hankeln, T.; Burmester, T.; Bolognesi, M. Human brain neuroglobin structure reveals a distinct mode of controlling oxygen affinity. *Structure* **2003**, *11*, 1087−1095.

(4) Dewilde, S.; Kiger, L.; Burmester, T.; Hankeln, T.; Baudin-Creuza, V.; Aerts, T.; Marden, M. C.; Caubergs, R.; Moens, L. Biochemical characterization and ligand binding properties of neuroglobin, a novel member of the globin family. *J. Bio. Chem.* **2001**, *276*, 38949−38955.

(5) Van Doorslaer, S.; Dewilde, S.; Kiger, L.; Nistor, S. V.; Goovaerts, E.; Marden, M. C.; Moens, L. Nitric oxide binding properties of neuroglobin. A characterization by EPR and flash photolysis. *J. Biol. Chem.* **2003**, *278*, 4919−4925.

(6) Hankeln, T.; Ebner, B.; Fuchs, C.; Gerlach, F.; Haberkamp, M.; Laufs, T. L.; Roesner, A.; Schmidt, M.; Weich, B.; Wystub, S.; Saaler-Reinhardt, S.; Reuss, S.; Bolognesi, M.; De Sanctis, D.; Marden, M. C.; Kiger, L.; Moens, L.; Dewilde, S.; Nevo, E.; Avivi, A.; Weber, R. E.;

Fago, A.; Burmester, T. Neuroglobin and cytoglobin in search of their role in the vertebrate globin family. *J. Inorg. Biochem.* **2005**, *99*, 110−119.
(7) Kakar, S.; Hoffman, F. G.; Storz, J. F.; Fabian, M.; Hargrove, M. S. Structure and reactivity of hexacoordinate hemoglobins. *Biophys. Chem.* **2010**, *152*, 1−14.
(8) Vallone, B.; Nienhaus, K.; Brunori, M.; Nienhaus, G. U. The structure of murine neuroglobin: Novel pathways for ligand migration and binding. *Proteins: Struct., Funct., Bioinf.* **2004**, *56*, 85−92.
(9) Tilton, R. F.; Kuntz, I. D.; Petsko, G. A. Cavities in proteins: Structure of a metmyoglobin xenon complex solved to 1.9 ANG. *Biochemistry* **1984**, *23*, 2849−2857.
(10) Vallone, B.; Nienhaus, K.; Matthes, A.; Brunori, M.; Nienhaus, G. U. The structure of carbonmonoxy neuroglobin reveals a heme-sliding mechanism for control of ligand affinity. *Proc. Natl. Acad. Sci. U.S.A.* **2004**, *101*, 17351−17356.
(11) Olson, J. S.; Phillips, G. N. Kinetic pathways and barriers for ligand binding to myoglobin. *J. Biol. Chem.* **1996**, *271*, 17593−17596.
(12) Anselmi, M.; Di Nola, A.; Amadei, A. Kinetics of Carbon Monoxide Migration and Binding in Solvated Neuroglobin As Revealed by Molecular Dynamics Simulations and Quantum Mechanical Calculations. *J. Phys. Chem. B* **2011**, *115*, 2436−2446.
(13) Nadra, A. D.; Marti, M. A.; Pesce, A.; Bolognesi, M.; Estrin, D. A. Exploring the molecular basis of heme coordination in human neuroglobin. *Proteins: Struct., Funct., Bioinf.* **2008**, *71*, 695−705.
(14) Bocahut, A.; Bernad, S.; Sebban, P.; Sacquin-Mora, S. Relating the diffusion of small ligands in human neuroglobin to its structural and mechanical properties. *J. Phys. Chem. B* **2009**, *113*, 16257−16267.
(15) Sun, Y.; Jin, K.; Mao, X. O.; Zhu, Y.; Greenberg, D. A. Neuroglobin is up-regulated by and protects neurons from hypoxic-ischemic injury. *Proc. Natl. Acad. Sci. U.S.A.* **2001**, *98*, 15306−15311.
(16) Hundahl, C.; Kelsen, J.; Kjær, K.; Rønn, L. C. B.; Weber, R. E.; Geuens, E.; Hay-Schmidt, A.; Nyengaard, J. R. Does neuroglobin protect neurons from ischemic insult? A quantitative investigation of neuroglobin expression following transient MCAo in spontaneously hypertensive rats. *Brain Res.* **2006**, *1085*, 19−27.
(17) Wang, X. Y.; Liu, J. X.; Zhu, H. H.; Tejima, E.; Tsuji, K.; Murata, Y.; Atochin, D. N.; Huang, P. L.; Zhang, C. G.; Lo, E. H. Effects of neuroglobin overexpression on acute brain injury and long-term outcomes after focal cerebral ischemia. *Stroke* **2008**, *39*, 1869−1874.
(18) Chan, A. S. Y.; Saraswathy, S.; Rehak, M.; Ueki, M.; Rao, N. A. Neuroglobin protection in retinal ischemia. *IOVS* **2012**, *53*, 704−711.
(19) Burmester, T.; Hankeln, T. What is the function of neuroglobin? *J. Exp. Bio.* **2009**, *212*, 1423−1428.
(20) Schmidt, M.; Giessl, A.; Laufs, T.; Hankeln, T.; Wolfrum, U.; Burmester, T. How does the eye breathe? Evidence for neuroglobin-mediated oxygen supply in the mammalian retina. *J. Biol. Chem.* **2003**, *278*, 1932−1935.
(21) Bentmann, A.; Schmidt, M.; Reuss, S.; Wolfrum, U.; Hankeln, T.; Burmester, T. Divergent distribution in vascular and avascular mammalian retinae links neuroglobin to cellular respiration. *J. Biol. Chem.* **2005**, *280*, 20660−20665.
(22) Guzy, R. D.; Hoyos, B.; Robin, E.; Chen, H.; Liu, L.; Mansfield, K. D.; Simon, M. C.; Hammerling, U.; Schumacker, P. T. Mitochondrial complex III is required for hypoxia-induced ROS production and cellular oxygen sensing. *Cell metabol.* **2005**, *1*, 401−408.
(23) Tiso, M.; Tejero, J. s.; Basu, S.; Azarov, I.; Wang, X.; Simplaceanu, V.; Frizzell, S.; Jayaraman, T.; Geary, L.; Shapiro, C.; Ho, C.; Shiva, S.; Kim-Shapiro, D. B.; Gladwin, M. T. Human neuroglobin functions as a redox-regulated nitrite reductase. *J. Biol. Chem.* **2011**, *286*, 18277−18289.
(24) Hamdane, D.; Kiger, L.; Dewilde, S.; Green, B. N.; Pesce, A.; Uzan, J.; Burmester, T.; Hankeln, T.; Bolognesi, M.; Moens, L.; Marden, M. C. The redox state of the cell regulates the ligand binding affinity of human neuroglobin and cytoglobin. *J. Biol. Chem.* **2003**, *278*, 51713−51721.
(25) Astudillo, L.; Bernad, S.; Derrien, V.; Sebban, P.; Miksovska, J. Probing the role of the internal disulfide bond in regulating conformational dynamics in neuroglobin. *Biophys. J.* **2010**, *99*, L16−L18.
(26) Nicolis, S.; Monzani, E.; Ciaccio, C.; Ascenzi, P.; Moens, L.; Casella, L. Reactivity and endogenous modification by nitrite and hydrogen peroxide: Does human neuroglobin act only as a scavenger? *Biochem. J.* **2007**, *407*, 89−99.
(27) Arcovito, A.; Moschetti, T.; D'Angelo, P.; Mancini, G.; Vallone, B.; Brunori, M.; Della Longa, S. An X-ray diffraction and X-ray absorption spectroscopy joint study of neuroglobin. *Arch. Biochem. Biophys.* **2008**, *475*, 7−13.
(28) Schmidt, M.; Nienhaus, K.; Pahl, R.; Krasselt, A.; Anderson, S.; Parak, F.; Nienhaus, G. U.; Srajer, V. Ligand migration pathway and protein dynamics in myoglobin: A time-resolved crystallographic study on L29W MbCO. *Proc. Natl. Acad. Sci. U.S.A.* **2005**, *102*, 11704−11709.
(29) Cohen, J.; Arkhipov, A.; Braun, R.; Schulten, K. Imaging the migration pathways for O_2, CO, NO, and Xe inside myoglobin. *Biophys. J.* **2006**, *91*, 1844−1857.
(30) Moschetti, T.; Mueller, U.; Schulze, J.; Brunori, M.; Vallone, B. The structure of neuroglobin at high Xe and Kr pressure reveals partial conservation of globin internal cavities. *Biophys. J.* **2009**, *97*, 1700−1708.
(31) Astudillo, L.; Bernad, S.; Derrien, V.; Sebban, P.; Miksovska, J. Conformational dynamics in human neuroglobin: Effect of His64, Val68, and Cys120 on ligand migration. *Biochemistry* **2013**, *51*, 9984−9994.
(32) Guimarães, B. G.; Hamdane, D.; Lechauve, C.; Marden, M. C.; Golinelli-Pimpaneau, B. The crystal structure of wild-type human brain neuroglobin reveals flexibility of the disulfide bond that regulates oxygen affinity. *Acta Crystallogr., Sect. D: Biol. Crystallogr.* **2014**, *70*, 1005−1014.